University Library



A gateway to Melbourne's research publications

Minerva Access is the Institutional Repository of The University of Melbourne

Author/s:
Gonzalez Viejo, C;Fuentes, S;Torrico, D;Howell, K;Dunshea, FR

Title:
Assessment of beer quality based on foamability and chemical composition using computer vision algorithms, near infrared spectroscopy and machine learning algorithms

Date:
2018-01-30

Citation:
Gonzalez Viejo, C., Fuentes, S., Torrico, D., Howell, K. & Dunshea, F. R. (2018). Assessment of beer quality based on foamability and chemical composition using computer vision algorithms, near infrared spectroscopy and machine learning algorithms. Journal of the Science of Food and Agriculture, 98 (2), pp.618-627. https://doi.org/10.1002/jsfa.8506.

Persistent Link:
https://hdl.handle.net/11343/293296

Fuentes Sigfredo (Orcid ID: 0000-0002-0377-5085)

030

Assessment of beer quality based on foamability and chemical composition using computer vision algorithms, near infrared spectroscopy and artificial neural networks modelling techniques.

Claudia Gonzalez Viejo [1], Sigfredo Fuentes [1]*, Damir Torrico[1], Kate Howell[1], and Frank R. Dunshea[1].

[1] University of Melbourne, School of Agriculture and Food, Faculty of Veterinary and Agricultural Sciences, VIC 3010, Australia

* Correspondence: sfuentes@unimelb.edu.au; Tel.: +61 3 9035 9670

Abstract

BACKGROUND

Beer quality is mainly defined by its color, foamability and foam stability, which are influenced by the chemical composition of the product such as proteins, carbohydrates, pH and alcohol. Traditional methods to assess specific chemical compounds are usually time-consuming and costly. This study used rapid methods to evaluate 15 foam and color-related parameters using a robotic pourer (RoboBEER) and chemical fingerprinting using near infrared spectrometry (NIR) from six replicates of 21 beers from three types of fermentation. Results from NIR were used to create partial least squares regression (PLS) and artificial neural networks (ANN) models to predict four chemometrics such as pH, alcohol, Brix and maximum volume of foam.

RESULTS

This is the author manuscript accepted for publication and has undergone full peer review but has not been through the copyediting, typesetting, pagination and proofreading process, which may lead to differences between this version and the Version of Record. Please cite this article as doi: 10.1002/jsfa.8506

This article is protected by copyright. All rights reserved.

The ANN method was able to create more accurate models (R = 0.95) compared to PLS. Principal components analysis using RoboBEER parameters and NIR overtones related to protein explained 67% of total data variability. Additionally, a subspace discriminant model using the absorbance values from NIR wavelengths resulted in the successful classification of 85% of beers according to fermentation type.

CONCLUSION

The method proposed showed to be a rapid system based on NIR spectroscopy and RoboBEER outputs of foamability that can be used to infer the quality, production method and chemical parameters of beer with minimal laboratory equipment.

Keywords: Beer chemometry; Robotic pourer; Multivariate data analysis; Artificial neural networks; Beer fermentation.

INTRODUCTION

Beer is defined as a yeast fermented beverage mainly composed of water, malted cereals and hops (1). Beer quality mainly depends on the combination of several factors such as the visual aspects, specifically color and foam-related attributes (foam stability, foam texture and bubble size), and its chemical composition, which are directly linked to sensory descriptors of beer for quality assessment (2). Amongst these chemical compounds and metrics related to quality

This article is protected by copyright. All rights reserved.

Author Manuscript

traits of beers are the protein and sugar types and content, alcohol, carbon dioxide concentration [CO_2], and pH (3, 4).

Beer manufacturing consists of a very complex process due to the numerous chemical reactions involved, which range from the malting of cereals (mainly barley) to the bottling of the final product including several steps such as mashing and boiling in between. It is critical to have the appropriate quality control and quality assurance measures of the final product, since any failure within the brewing process could result in the development of off-flavors and / or undesired visual characteristics such as the lack of foaming, and [CO_2] for bubble and foam stability and haze formation, among others (5).

Beers can be produced through three major types of fermentation (top, bottom and spontaneous), which have several variations within their specific process, such as the type of yeast used, the production temperature and the fermentation time. Top fermentation beers are usually produced within five days by using yeast such as *Saccharomyces cerevisiae,* which is added at temperatures between 15 and 25 °C and is able to ferment through an aerobic process that allows it to remain in the surface of the liquid. Conversely, the bottom fermenting process can take from seven days up to several weeks and generally uses *S. carlbergensis* as the fermenting yeast, which is added at temperatures within the 6

Author Manuscript

This article is protected by copyright. All rights reserved.

– 8 °C range and is able to act anaerobically by settling on the bottom of the container. Finally, spontaneous fermentation consists of a longer brewing process that can last up to two years. Beer is fermented aerobically at temperatures around 16 °C by using wild yeast and bacteria present in the environment where it is produced (6).

During beer fermentation, the alcohol and sugar content are defined, and depend mainly on the level of flocculation and attenuation of the yeast. Hence, the production of beers with higher sugar and lower alcohol content is provided by the fast-flocculating yeasts, with low attenuation. On the other hand, high quality beers with higher alcohol content and lower sugar concentrations, are obtained by the addition of slow flocculating yeasts with high attenuation. During this sugar to ethanol conversion other chemical changes occur, as CO_2 is released, pH decreases from pH 5.5 to around pH 4.3 and nitrogen (N_2) content is reduced by one third, while most of the hop resins are lost, leaving traces that are responsible for the bitter taste of the final product (2, 7, 8).

The gas dissolved in beer, which mainly consists of CO_2 and N_2, is the main component responsible for the foam formation and bubble size once it is released, when the beer bottle is opened and poured to a glass. This occurs when the gas rises in the form of bubbles due to a reduction in pressure forming a thin layer in

Author Manuscript

This article is protected by copyright. All rights reserved.

the interphase liquid – gas called lamella (9). The latter process of foam formation is possible due to the surfactant substances, such as proteins and sugars, present in the surface of the beer, which are able to increase the viscosity of the liquid and reduce the rate of drainage of the lamella. The pH also plays an important role for foam formation and stability because as the proteins are closer to their isoelectric pH, they tend to be more stable and decrease the pressure of repulsion connections, which promotes more favorable interactions between the proteins and the formation of viscous films in the interphase (5, 10). Foam acts as a protecting layer to avoid the oxidation of the beer and thus preventing the formation of off-flavors during its consumption (11, 12).

Therefore, it is essential also to analyze the intrinsic factors of beers, such as protein and sugar contents to find their relationship with the foam stability parameters. Current methods to assess quality components are costly and time-consuming, as they involve the use of skilled technicians, expensive laboratory equipment and facilities to carry out all the samples preparation and tests needed to get the desired parameters. The official method to analyze protein in beer is the Kjeldahl method (AOAC 920.53 – 1978). This method measures the total crude protein based on the amino nitrogen content and does not quantify the specific proteins that contribute to foam stability. Other methods that have been used in

Author Manuscript

This article is protected by copyright. All rights reserved.

previous studies are the Biuret, in which the hops present in the beer interfere with the ultraviolet light readings. Furthermore, the Bradford assay is unable to react with proteins containing glutamic acid and proline making it difficult to determine their concentration (13). For these reasons, some authors have found that isolating the proteins from beer, usually by precipitation, and the use of immunological techniques such as ELISA and electrophoresis methods could render more accurate protein analysis (5, 14, 15). Nonetheless, these techniques are also time consuming, require skilled personnel and the use of specialized laboratory material and instrumentation.

Since most of the simple sugars are transformed into alcohol by yeast during fermentation, most the carbohydrates present in beer are oligo- and polysaccharides. Some of the oligosaccharides that have been studied are the β-glucans by using an assay kit from Megazime, and the malto-oligosaccharides using high-performance liquid chromatography (HPLC) techniques (4, 16). However, these methods are more complex, less cost effective and require more time for sample preparation.

Novel techniques to assess beer chemometry, which involve non-linear methods have been used by other authors such as Cajka et al. (17) that developed predictive models using partial least squares (PLS), linear discriminant analysis and

Author Manuscript

This article is protected by copyright. All rights reserved.

artificial neural networks (ANN) for different gas chromatography and head space methods to obtain volatile fingerprinting from beer with results showed higher accuracy using ANN. Other authors such as Iñón et al. (18) compared PLS and ANN methods obtaining better results with ANN using combined mid and near infrared to determine quality parameters of beer based on alcohol content and real extract. In this case, ANN modelling was also used in beer research for prediction of acetic acid (19). Another method suggested as being efficient for non-linear modelling is the locally weighted regression (LWR) that has been used for prediction of beer chemometry during fermentation (20), however, this method has as disadvantage that it requires a new calibration every time a new sample needs to be analyzed (21).

This paper discusses the assessment of foaming properties of beer samples from three different types of fermentation using RoboBEER, which is a newly developed robotic pourer coupled with computer vision algorithms (2). A near infrared spectroscopy (NIR) handheld was used to obtain the chemical fingerprinting of beers to assess the influence of beer compounds on foaming properties by their characteristic levels of absorbance or overtones. This paper also presents prediction models obtained using both partial least squares (PLS) regression and the artificial neural networks (ANN) fitting tool in Matlab®. Soluble

Author Manuscript

This article is protected by copyright. All rights reserved.

solids content, the maximum volume of foam, pH and alcohol content using the specific values of absorbance in the NIR spectra and data from the RoboBEER were used as inputs and chemometry as targets. Therefore, the objective of this research was to develop an effective method and find an accurate model to ease the assessment of beer quality based on foamability using the RoboBEER, by comparing two different regression techniques. Furthermore, a classification subspace discriminant model was developed to group the beers according to the type of fermentation using their chemical fingerprinting as inputs.

MATERIALS AND METHODS

Beer Samples

For this study, eight samples from top, seven from bottom and six from spontaneous fermentation produced in different countries were used (Table 1). Specific beers were selected to broaden the range of results for the foamability properties as well as chemometrics to be able to find representative relationships among them and specific models that can be applied to new samples. To take into account sampling variability, six replicates (six bottles per beer sample) from two different batches, three bottles of each batch, purchased in 2015 and 2016 were used for all the analyses. The measurements of the two batches were carried out in

Author Manuscript

This article is protected by copyright. All rights reserved.

two different dates and all parameters were measured from the same bottles the in the same day to avoid any compositional modifications due to the influence of oxygen contact with the beer.

Table 1 List of beer samples analyzed, showing the type of beer, classification according to their type of fermentation, country of origin, the abbreviated label used for their identification for all the analyses performed, color of bottle and type of seal.

Type/Subtype	Country of Origin	Label	Bottle color	Seal
Top Fermentation				
Abbey Ale	Belgium	L	Brown	Bottle cap
India Pale Ale	Australia	IP	Brown	Bottle cap
Porter	Poland	Z	Brown	Bottle cap
Kolsch	Australia	P	Brown	Bottle cap
Red Ale	USA	RT	Brown	Bottle cap
Steam Ale	Australia	SA	Brown	Bottle cap
Aged Ale	Scotland	IG	Brown	Bottle cap
Sparkling Ale	Australia	CS	Brown	Bottle cap
Bottom Fermentation				
Lager	Mexico	C	Clear	Bottle cap
Lager	Mexico	XX	Green	Bottle cap
Lager	USA	BL	Brown	Bottle cap
Lager	Netherlands	H	Green	Bottle cap
Lager	Czech Republic	BC	Green	Bottle cap
Lager Low Alcohol	Germany	BB	Green	Bottle cap
Pilsner	Czech Republic	PU	Green	Bottle cap
Spontaneous Fermentation				
Lambic Cassis	Belgium	LC	Green	Cork + Bottle cap
Lambic Framboise	Belgium	LF	Green	Cork + Bottle cap

Author Manuscript

This article is protected by copyright. All rights reserved.

Lambic Gueuze	Belgium	LG	Green	Cork + Bottle cap
Lambic Kriek	Belgium	LK	Green	Cork + Bottle cap
Lambic Kriek	Belgium	OK	Green	Cork
Lambic Gueuze	Belgium	OG	Green	Cork

Total soluble solids, alcohol and pH measurements

Total soluble solids from all samples and replicates were measured in degrees Brix (Brix) using an optical refractometer Alla France REFBX010 (Alla France Sarl, Chemillé-Melay, France) with a range of measurement of 0 – 32 Brix. All samples were measured at room temperature (23 – 25 °C) and the refractometer was rinsed with distilled water and dried between each measurement to avoid cross-contamination. The pH was measured with a pH-meter HANNA HI9025 (Hanna Instruments Canada Inc. Laval, QC. Canada). The equipment was calibrated by using buffer solutions at pH 4.0 and 7.0. A 50 mL beaker was used to test samples by pouring the same sample amount from each beer (50 mL) at temperatures within the 23 – 25 °C range. The alcohol content was measured with an Alcolyzer Wine M alcohol meter (Anton Paar GmbH, GRAZ, Austria) set to use the wine extension method included in the Alcolyzer settings (Alcolyzer WineM manual), all samples were previously degassed using a vacuum pump and a magnetic stirrer at ambient temperatures between 23 – 25 °C.

Near infrared spectroscopy

Author Manuscript

This article is protected by copyright. All rights reserved.

Beer sample spectra was measured right after the foam-related parameters were measured using a handheld microPHAZIR™ RX Analyzer (Thermo Fisher Scientific, Waltham, MA. USA). This device is capable of measuring the spectra, which can be related to a chemical fingerprint of materials by reading the absorbance of different wavelengths within the 1600 – 2396 nm (every 7 – 9 nm) range. To standardize measurements, a filter paper Whatman® (Whatman plc. Maidstone, United Kingdom) qualitative grade three and 7.0 cm was used as the media to contain the liquid samples. Before starting the first set of measurements and after every 10 – 15 readings, the equipment was calibrated by using a white background (included with the device), which turns the lamp on to avoid variations in the light as well as in any environmental changes. The measurement procedure for all samples consisted in reading the dry filter paper by itself without samples first to be able to subtract the absorbance values from the beer samples readings. After this procedure, the filter was submerged in the specific sample and placed on the 5 mm measuring region at the front of the NIR device. All readings were performed placing the white background at the back with the filter in between (with and without samples) to avoid signal noise inclusion due to environmental factors. The filter, once soaked with the sample, was measured immediately (within 5 seconds) to avoid any loss of volatile compounds. Readings were performed in

Author Manuscript

This article is protected by copyright. All rights reserved.

triplicates from each sample to reduce variation and all samples were also measured at room temperature (20 – 23°C).

To validate the filter paper method, a simple test using pure water and ethanol 100% undenatured was performed by following the same procedure as the beer sample measurements. Furthermore, a simple comparison between the filter paper method and the one proposed by Thermo Fisher Scientific using silica as media was performed. The Thermo Fisher method uses 4 mL vials and silica sand as the media to diffuse the liquid samples; this compound is used due to its low reactivity and low reflective index. To measure the sample, 1.25 mL of silica sand was added to the vial along with 2 mL of the liquid and they were mixed by shaking the vial. The latter was then inserted in the adapter of the device and measured the same way as with the filter method. A graph was generated to compare the two methods used to measure NIR using the absorbance values of the whole spectra of the silica method and the extracted values of beer from the filter method to find the correlation between both of them. To assess the accuracy of the results, statistical data was obtained, such as determination coefficients (R^2), error sum of squares (SSE), root mean square error (RMSE) and p-value using the curve fitting toolbox in Matlab® ver. 2016a (Mathworks Inc., Matick, MA. USA).

Author Manuscript

This article is protected by copyright. All rights reserved.

Foaming parameters description

The foaming parameters were the first measurement for all the samples to achieve minimal loses of CO_2 within the time between opening and pouring (~30 s). All 15 foaming parameters were obtained using RoboBEER, which consists of a robotic pourer for beer samples capable of measuring CO_2 released when pouring, pouring temperature and alcohol content in real time using three integrated sensors controlled with Arduino® boards (Arduino, Italy). RoboBEER is able to record videos of the samples for five minutes starting just before pouring by using a smartphone, which are analyzed using customized codes based on computer vision algorithms written in Matlab®. A detailed description of the RoboBEER and the method used can be found in Gonzalez Viejo et al. (2). The analysis codes were designed to obtain the most relevant foaming parameters such as the maximum volume of foam (MaxVol), total lifetime of foam (TLTF), lifetime of foam (LTF), foam drainage (FDrain), bubbles size count grouped by small, medium and large, and color descriptors using two different color scales (RGB and CieLab), the description of these measurements are shown in Table 2.

Table 2 Description and abbreviation of all foaming parameters obtained with RoboBEER.

Author Manuscript

This article is protected by copyright. All rights reserved.

Parameter (units)	Abbreviation	Description
Total lifetime of foam (s)	**TLTF**	Lifetime of foam for the whole period (5 mins).
Lifetime of foam (s)	**LTF**	Lifetime of foam starting from the volume peak as the area below the curve.
Maximum volume of foam (mL)	**MaxVol**	Maximum volume of foam.
Foam Drainage (mL s^{-1})	**FDrain**	The excess of beer drained from the wet foam to give dry foam.
Alcohol sensor (unitless)	**OH**	Ethanol gas of the sample measured with the sensor.
Carbon dioxide (ppm)	**CO_2**	CO_2 content measured with the sensor.
CieLab color scale (unitless)	**L, a and b**	Color parameters in CieLab scale where: L is lightness, a represents the red and green values and b the yellow and blue values.
RGB color scale (unitless)	**RI, GI and BI**	Color parameters in RGB scale converted to color index where: RI represents the red intensity ratio, BI the blue intensity ratio and GI the green intensity ratio. Values obtained with the following equations: RGB intensity ratio (I) =R+G+B Red intensity ratio (RI) = R/I Green intensity ratio (GI) = G/I Blue intensity ratio (BI) = B/I
Small bubbles (number)	**SmBubb**	Number of small bubbles in the foam.
Medium bubbles (number)	**MedBubb**	Number of medium bubbles in the foam.
Large bubbles (number)	**LgBubb**	Number of large bubbles in the foam.

Author Manuscript

This article is protected by copyright. All rights reserved.

Statistics from chemical analysis of beers

Averaged data from replicates were analyzed obtaining standard deviation of the samples (SD) to assess the variability between the different bottles of each beer (Table S1 and S2). A high variability between the replicates was found for all foam related parameters (MaxVol, TLTF, LTF, OH, CO_2, SmBubb, MedBubb, LgBubb and FDrain) due to differences in sealability between bottles, especially for capped beers as expected and explained previously by Gonzalez Viejo et al. (2). Due to this variability, the mean values of the six bottles were used for the multivariate data analysis.

NIR data analysis

Data obtained from the NIR device were analyzed using The Unscrambler X ver. 10.3 (CAMO Software, Oslo, Norway) software. This statistical program was able to plot the absorbance values found for all wavelengths for each sample. Additionally, the partial least squares (PLS) regression method was used for pH, degree Brix, alcohol and MaxVol to develop a predictive model with each of those metrics as targets and the NIR values as inputs. To create these models a non-linear iterative partial least squares (NIPALS) algorithm was used. The data used to create the models did not undergo any transformation to be comparable with those

Author Manuscript

This article is protected by copyright. All rights reserved.

using ANN. This method works by randomly using the total number of samples (n) for both calibration and validation. Statistical data such as the determination coefficients (R^2), slope and root mean square error (RMSE) were used to assess model performance.

Multivariate data analysis, artificial Neural Network (ANN) modelling and classification

A multivariate data analysis based on principal components analysis (PCA) and cluster analysis was performed for all data obtained in this study by using a customized code written in Matlab® (Fuentes, unpublished). The cluster analysis is used to identify patterns within all values to classify the samples and the PCA can be used to find relationships between all parameters.

The ANN fitting tool from Matlab Neural Network Toolbox™ 7 (Mathworks Inc., Matick. MA. USA) was used to obtain specific prediction models using the Levenberg-Marquardt training algorithm. Four models were created with different targets such as MaxVol, degrees Brix, pH and alcohol content using specific spectra overtone readings from the NIR as inputs (Figure 1). Overtones within the 2177 – 2396 nm range were used as inputs for MaxVol, whilst values between 2001 and 2270 nm wavelength range were used for Brix and the whole spectra (1600 – 2396

Author Manuscript

This article is protected by copyright. All rights reserved.

nm) for pH and alcohol. The selection of the wavelength ranges for MaxVol and Brix was done according to Burns (21), which identifies most of the protein overtones corresponding to the 2177 and 2396 nm range and carbohydrates are mainly within 2000 and 2271 nm. Furthermore, a general model using the whole NIR spectra (1600 – 2396 nm) was created using the four targets (MaxVol, Brix, pH and alcohol content). The artificial neural networks data division works dividing the data into three stages: i) Training, which is necessary to compute the gradient and to update the weights and biases, ii) Validation, which is needed to minimize the error and ovoid overfitting by monitoring the validation error in the training stage, and iii) Testing, which is necessary to compare different models. Therefore, for all the models, a random data division using the *dividerand* function in Matlab was used, which randomly divides the data from samples into the three stages with 70% (n = 45) for training, 15% (n = 9) for validation with a mean squared error performance algorithm and 15% (n = 9) for testing with a default derivative function, the data used in each stage is not used in the other two, this makes every stage independent from each other. Three hidden neurons were used for the five models (specific and general) and different wavelengths were added as inputs for each model according to the selected target (Figure 1). The four models for the individual targets were used to compare the ANN statistical model performance

Author Manuscript

This article is protected by copyright. All rights reserved.

results with those from the PLS regression. To assess and compare the accuracy of the results from the two models tested (PLS and ANN), statistical data such as the determination coefficients (R^2), slope (Sl) and root mean square error (RMSE) were obtained. There was no outlier analysis for any of the fitting models presented, hence models include all the data from replicates and beer samples.

Figure 1 Two-layer feedforward network with three hidden neurons and sigmoid functions to fit regression models for targets and inputs: (a) maximum volume of foam (MaxVol) using the 2177 and 2396 nm wavelength range (n = 30), (b) Degrees Brix (Brix) with near infrared (NIR) wavelengths within the 2001 and 2270 nm range (n = 35), and (c) pH and (d) alcohol both using all NIR spectra (n = 100), and (e) model using the four chemometric analyses as targets and the all NIR as inputs. Three hidden neurons were chosen for the four models using Matlab ver. 2016a (Mathworks Inc., Matick, MA. USA). For hidden and output layers, w = weights and b = biases.

Additionally, a classification model using the subspace ensemble method and the discriminant learner type was created using the Matlab® Classification Learner application in the Statistics and Machine Learning Toolbox™ (Mathworks Inc.,

This article is protected by copyright. All rights reserved.

Matick. MA. USA) to classify beers according to fermentation type. The whole NIR absorbance values corresponding to the range of wavelengths within 1600 and 2396 nm (n = 100) were used as inputs in the ANN as beer chemical fingerprinting. A total of 30 learners and a value of 50 for the subspace dimension were used to train the model.

RESULTS

Near infrared spectrometer method validation

Figure 2 shows the graph of NIR measurements for water and pure ethanol using the filter paper method for standardization purposes. In this figure, the higher peaks for the dry filter (red line) corresponded to the range of cellulose and starch overtones with corresponding to values between 1880 – 1993 nm and 2000 – 2396 nm (21). As further shown in this figure, after subtracting the filter values, the peak of water overtones (1940 nm) (22) was enhanced and the absorbance in the wavelengths corresponding to cellulose and starch overtones were minimized (blue line). Similarly, the ethanol curve (green line) shows the peak values for the absorbance around the wavelengths corresponding to alcohol overtones (2090, 2270 and 2304 nm) (21, 23).

Author Manuscript

This article is protected by copyright. All rights reserved.

Figure 2 Absorbance curves (y axis) obtained for the wavelength spectra in nm (x axis) measured with the NIR device for ethanol (green line), dry filter (red line), filter with ethanol (black line), filter with water (purple line) and water (blue line).

As shown in Figure 3 the measurements made for five different samples, representing the three fermentation types and using the whole spectra for both the filter paper (x axis) and the silica sand (y axis) presented similar errors, with consistent difference values (50 - 52%) and high correlation between the two methods. This test showed that both methods are equivalent for benchmarking purposes. The measurements were made with samples H, LC, CS, BL and Z obtaining R^2 values of 0.97 (SSE = 0.23; RMSE = 0.05; p-value = < 0.0001), 0.92 (SSE = 0.55; RMSE = 0.08; p-value = < 0.0001), 0.91 (SSE = 0.76; RMSE = 0.09; p-value = < 0.0001), 0.83 (SSE = 1.14; RMSE = 0.11; p-value = < 0.0001) and 0.92 (SSE = 0.48; RMSE = 0.07; p-value = < 0.0001), respectively.

Figure 3 Curves representing the correlation between the beer measured with the filter paper (x axis) and beer measured with the silica sand (y axis) methods comparing values of the whole wavelength spectra obtained. Each curve represents a different sample as specified in the graph. The abbreviations of the samples are shown in Table 1.

Author Manuscript

This article is protected by copyright. All rights reserved.

Near infrared spectrometry results

Figure 4 shows the graphs for the averages from replicates from each brand of beer. Each group of beers, according to the type of fermentation, is represented with a different color: purple for spontaneous, blue for top and green for bottom fermentation. As observed in this figure, the peak values for all beers are within the range of ~1850 – 2000 nm, in which compounds such as alcohol, water, proteins, urea, carbohydrates and volatiles such as amides can be found (21).

Figure 4 Curves of all beer samples showing the absorbance values (y axis) for all wavelengths (x axis) in the NIR spectra reported in nm. Each group of beers is represented with a different color: green for bottom, blue for top and purple for spontaneous fermentation.

Table 3 shows the summary of results from both regression models (PLS and ANN) generated for four chemical components as targets (MaxVol, Brix, pH and Alcohol). The ANN regression models were able to fit the targets more accurately than the PLS regression models as the ANN had higher R^2 and lower RMSE values in both calibration / training and validation stages. PLS regression models are only able to generate calibration and validation curves, thus training and overall values are only shown for ANN models.

Author Manuscript

This article is protected by copyright. All rights reserved.

Table 3 Comparison of results obtained from the regression model using both partial least squares regression (PLS) and artificial neural networks (ANN) for four chemical components. Results presented for each stage of the models are the determination coefficient (R^2), root mean squared error (RMSE) and slope (Sl). The blank cells are denoted as a hyphen (-) since PLS does not generate those results. The general model outputs, which include maximum volume of foam (MaxVol), Brix, pH and Alcohol as combined targets, are only from the ANN modelling.

Target	Model	Calibration / Training			Validation			Testing			Overall		
		R^2	RMSE	Sl	R^2	RMSE	Sl	R^2	RMSE	Sl	R^2	RMSE	Sl
1	**PLS**	0.67	10.69	0.67	0.54	12.74	0.58	-	-	-	-	-	-
MaxVol	**ANN**	0.93	5.05	0.98	0.77	9.61	0.92	0.82	10.59	1.32	0.85	7.60	1.01
2	**PLS**	0.79	0.95	0.79	0.71	1.12	0.75	-	-	-	-	-	-
Brix	**ANN**	0.91	0.60	0.99	0.86	0.87	1.01	0.74	1.15	1.00	0.87	0.74	0.99
3	**PLS**	0.70	0.30	0.70	0.64	0.32	0.64	-	-	-	-	-	-
pH	**ANN**	0.95	0.21	0.98	0.80	0.12	1.00	0.83	0.25	1.02	0.91	0.17	0.99
4	**PLS**	0.88	0.01	0.88	0.85	0.01	0.85	-	-	-	-	-	-
Alcohol	**ANN**	0.99	0.01	0.99	0.92	0.002	1.00	0.89	0.01	0.97	0.97	0.003	0.99
All four targets	**ANN**	0.97	0.12	0.97	0.87	0.21	0.89	0.95	0.14	0.92	0.95	0.14	0.95

Figure 5a shows the overall ANN regression model for four chemical components (MaxVol, Brix, pH and Alcohol) used as targets using the 126 samples. This graph was obtained using the data from the three ANN modelling processes of training, validation and testing. It can be observed that the model using the four targets had a high correlation and low error values (R^2 = 0.95, RMSE = 0.14, slope = 0.95), and most of the data points were fitted to the regression line.

Author Manuscript

This article is protected by copyright. All rights reserved.

Furthermore, the error histogram for the model had a normal distribution (Figure 5b).

Figure 5 Results from Artificial Neural Networks (ANN) showing (a) the overall regression model using the 126 samples with four targets: i) maximum volume of foam (MaxVol) ii) total soluble solids (Brix) iii) pH values and iv) alcohol content. The values from the whole NIR wavelength range (1596 – 2396 nm) were used as inputs. Predicted values are shown in y axis, while observed values can be observed in x axis. (b) The error histogram showing a trend of normal distribution in which the x – axis represents the errors calculated as observed minus estimated.

RoboBEER and NIR

Figure 6a shows the principal components analysis of all parameters measured with RoboBEER and the absorbance values of the 2300 nm wavelength, which represents the second overtone of protein (NIRP) (21). As seen in this figure, the principal component 1 (PC1) represented 45% of data variability, while the principal component 2 (PC2) accounted for 22%, hence 67% of the total variability is explained by the PCA. The absorbance values for protein measured with NIR (NIRP) had a positive correlation with most foaming parameters (MaxVol, TLTF, LTF, SmBubb) and OH. Conversely, these parameters were negatively related with

Author Manuscript

This article is protected by copyright. All rights reserved.

FDrain. On the other hand, Brix was positively related with RI, a and b, MedBubb and LgBubb, and had a negative relationship with GI, BI, L and pH. Figure 6b shows that the cluster analysis was able to separate most of the beers into three clusters according to their type of fermentation.

Figure 6 Results from the multivariate data analysis: (a) PCA for all foaming parameters measured with RoboBEER and absorbance values for 2300 nm NIR values corresponding to protein overtones (NIRp), and (b) cluster analysis according to the type of fermentation (green squares: bottom, blue circles: top, and purple triangles: spontaneous). Green descriptors in vectors represent the foam-related parameters, pink letters represent the color parameters, the red ones depict the sensors readings form the RoboBEER and brown descriptors represent the chemometrics and NIR values.

Table 4 shows the overall results obtained from the model created using a subspace discriminant method. The confusion matrix shows that there was an 85% accuracy when classifying beers according to their type of fermentation using the absorbance values obtained with NIR measurement. Several retraining attempts were made using different number of learners to validate the accuracy of the model and all these were consistent obtaining similar results.

Author Manuscript

This article is protected by copyright. All rights reserved.

Table 4 All confusion matrix for the 126 bottles of beer analyzed using a subspace discriminant method for the three types of fermentation. The first from each set of numbers corresponds to the number of samples and the second line shows the percentage from total samples. Values in italics correspond to the number of sample misclassification with associated errors.

Fermentation	Bottom	Spontaneous	Top	Overall
Bottom	31	*2*	*9*	
	82%	*5%*	*18%*	
Spontaneous	*0*	36	*0*	
	0.0%	92%	*0.0%*	
Top	*7*	*1*	40	
	18%	*3%*	82%	
Accuracy	82%	92%	82%	**85%**
Error	*18%*	*8%*	*18%*	***15%***

Figure 7 shows the receiver operating characteristic (ROC) curve, which displays the location of the classifier tested (orange dot) within the true positive rate values. Furthermore, an area under the curve of 0.88 was obtained.

Figure 7 Curve showing the receiving operator characteristic (ROC), where the orange circle represents the classifier, which is closer to the top left edge for true positive rate values. The value for area under the curve is also shown.

DISCUSSION

Near infrared spectrometer media (filter paper versus silica)

This article is protected by copyright. All rights reserved.

The results obtained by measuring pure water and ethanol showed that the filter paper method was effective to get accurate results from the NIR spectrometer for benchmarking purposes. This method allowed consistent isolation of the values of the filter to get only the results from the liquid sample (Figure 2). Furthermore, from the comparison between the filter paper and silica sand methods, it was found that they were highly correlated and, despite that the filter paper method underestimates the sand media absorbance, this trend is similar for all the samples. The overestimation found in the silica method can be attributed to its high liquid absorption capacity as well as to its light transmission properties (24, 25). Hence, both validation methods (Figure 2 and 3) showed that the use of filter paper could effectively replace the current methods recommended by the suppliers that usually represent high costs.

Near infrared spectroscopy

The NIR absorbance scan for beer samples from top and bottom fermentation followed a similar trend among each other, while the spontaneous fermentation beers presented a different signal shape above 2200 nm (Figure 4). Spontaneous fermentation beers had an increase of absorbance above the above-mentioned wavelength in which compounds such as protein, carbohydrates and oils are present. For all beer samples, the main chemical component fingerprinting was

Author Manuscript

This article is protected by copyright. All rights reserved.

achieved using the NIR handheld device, and these compounds likely involve aromatics such as amides, proteins, alcohol, carbohydrates, water and some hop oils (21). Similar curve trends within the same wavelength range of NIR measurements of different types of wine samples have been obtained by other authors such as Urbano-Cuadrado et al. (26) and Manley et al. (27). This is comparable to our results, since wine and beer are both fermented alcoholic beverages that, although in different proportions, are mainly composed of water, alcohol and residual sugars.

When generating models using both PLS and ANN regression, it was found that ANN was more capable of fitting the target values to the inputs / predictors (NIR absorbance values), as they presented higher R^2 and lower error values than the PLS regression models for both calibration, training and validation stages (Table 3). Similar findings from the comparison between PLS and ANN models have been published by other authors working on beer modelling (17, 18). Unlike the PLS regression the ANN fitting tool works using machine learning algorithms, which simulate the brains processing techniques and is able to find complex non–linear relationships among inputs and targets. Furthermore, ANNs are able to generate three stages for model development: training, validation and testing, which makes the final model more robust and reliable avoiding overfitting (28).

Author Manuscript

This article is protected by copyright. All rights reserved.

As expected, the range of wavelengths between 2177 – 2396 nm, which characterizes most of the proteins and carbohydrates spectra ranges and overtones, had a high correlation with the MaxVol in the specific ANN regression model (Table 3). This can be attributed to the influence that proteins and carbohydrates have on the formation and stabilization of foam in beer, especially high molecular weight proteins (>10 kDa) and polysaccharides (5, 29). These models showed that the NIR analyzer used is able to predict accurately the MaxVol of different beers through ANN modelling.

The selected wavelengths between 2001 and 2270 nm, are characterized mainly by carbohydrates (21), and had a moderately high correlation with Brix (Table 3). This is in accordance with a study with grapes in which Parpinello et al. (30) used the wavelength region around 2170 nm to predict soluble solids content measured in Brix and found a high overall correlation in the specific ANN model (R^2 = 0.87). Although beer as a final product does not have a high sugar content, the fact that yeasts are not able to consume all simple sugars and its inverse relationship with alcohol content, rely on the presence of residual sugars in beer (8).

Models for both pH and alcohol content were developed using the whole NIR spectra and created the best specific prediction models (Table 3). The alcohol

This article is protected by copyright. All rights reserved.

content was expected to present a good regression model as the equipment (Alcolyzer) used to measure the real values works with near infrared spectroscopy. However, the PLS regression was not able to create a model as accurate as the ANN method. Other authors have developed accurate prediction models using NIR for ethanol content in beer (18) and ethanol and pH in wine (26).

The general ANN regression model created using the absorbance values from the whole wavelength range (1596 – 2396 nm) as inputs and the four components combined (MaxVol, Brix, pH and alcohol) as targets showed to be highly accurate with an overall R^2 = 0.95 (Figure 5). This method showed to be more efficient as all four targets can be obtained in a single. Model using the whole spectra, apart from the capability of the method of being fed with new data to predict the numerical and objective valued of each target.

RoboBEER and near infrared spectroscopy, and classification modelling

Proteins play a very important role in beer foamability, as these are able to permeate into the walls of bubbles and thus improve foam formation. Moreover, proteins can increase the viscosity of both the bulk and surface liquids, which increases the foam stability of the beer and reduces the foam drainage. This could explain the positive correlation found between NIRP and foaming parameters such

This article is protected by copyright. All rights reserved.

as MaxVol, TLTF, LTF and SmBubb, and the negative relationship with FDrain. The positive relationship between Brix and red color (a and RI) can be attributed to the addition of red fruit juice to the flavored spontaneous fermentation beers, which resulted in higher sugar content and presented higher values of red color. Additionally, Abeytilakarathna et al. (31) found a correlation between Brix and red, blue and green colors in fruits, which supports findings presented in this paper.

The subspace discriminant model developed using the absorbance values of 100 NIR wavelengths showed to be highly accurate with 85% positive classification of beers according to the type of fermentation. Most of the misclassifications were found between top and bottom fermentation beers, which represent variation in the fermentation process and type of yeast, but share some similarities in characteristics such as alcohol content, pH and Brix. However, the model developed showed that the method used to measure NIR in beer was adequate to obtain the chemical fingerprinting of these samples and that it was able to identify differences in chemical composition of beers within the different types of fermentation.

CONCLUSIONS

The methodology proposed in this paper showed that accurate prediction models could be developed using robotics, computer vision NIR spectroscopy and machine learning algorithms to assess chemical and physical quality traits from

Author Manuscript

This article is protected by copyright. All rights reserved.

beer. The NIR based models could allow rapid screening of beers to objectively assess the main quality traits related to foamability and chemical properties. Furthermore, specific overtones in the NIR spectra of beers related to protein content were correlated to foaming properties of beers, which can result in the development of simple modelling strategies to assess chemometry of beers based on computer vision algorithms. Therefore, the method proposed showed to be a rapid system based on NIR spectroscopy and RoboBEER outputs of foamability that can be used to infer the quality, production method and chemical parameters of beer with minimal laboratory equipment. However, further research involving the analysis of proteomics would allow to create a more robust and specific model that includes specific proteins which are the main components responsible for foam formation and stability.

ACKNOWLEDGEMENTS

This research was partially funded by the Australian Government through the Australian Research Council [Grant number IH120100053] 'Unlocking the Food Value Chain: Australian industry transformation for ASEAN markets'.

REFERENCES

1. Caballero I, Blanco CA, Porras M. Iso-α-acids, bitterness and loss of beer quality during storage. Trends in Food Science & Technology. 2012;26(1):21-30.
2. Gonzalez Viejo C, Fuentes S, Li G, Collmann R, Condé B, Torrico D. Development of a robotic pourer constructed with ubiquitous materials, open

This article is protected by copyright. All rights reserved.

hardware and sensors to assess beer foam quality using computer vision and pattern recognition algorithms: RoboBEER. Food Research International. 2016.
3. Cooper DJ, Husband FA, Mills ENC, Wilde PJ. Role of Beer Lipid-Binding Proteins in Preventing Lipid Destabilization of Foam. Journal of Agricultural and Food Chemistry. 2002;50(26):7645-50.
4. Ferreira IMPLVO, Jorge K, Nogueira LC, Silva F, Trugo LC. Effects of the Combination of Hydrophobic Polypeptides, Iso-α Acids, and Malto-oligosaccharides on Beer Foam Stability. Journal of Agricultural and Food Chemistry. 2005;53(12):4976-81.
5. Bamforth C, Russell I, Stewart G. Beer: A Quality Perspective: Elsevier Science; 2011.
6. Papadopoulou-Bouraoui A, Vrabcheva T, Valzacchi S, Stroka J, Anklam E. Screening survey of deoxynivalenol in beer from the European market by an enzyme-linked immunosorbent assay. Food additives and contaminants. 2004;21(6):607-17.
7. Soares EV. Flocculation in Saccharomyces cerevisiae: a review. Journal of Applied Microbiology. 2011;110(1):1-18.
8. Delcour JA, Hoseney RC. Principles of Cereal Science and Technology: AACC International; 2010.
9. Zhang Y. Geochemical Kinetics: Princeton University Press; 2008.
10. Badui S. Química de los Alimentos. México: Pearson Education; 2006.
11. Ortiz FG, Muela MG, Ortiz PPG. Bebidas: Thomson Paraninfo; 2003.
12. Thomsen JPA. Pasión, Espumas y Anécdotas: Jörg P.A. Thomsen; 2007.
13. Londesborough J, Dresel M, Gibson B, Juvonen R, Holopainen U, Mikkelson A, et al. Analysis of Beers from an 1840s' Shipwreck. Journal of Agricultural and Food Chemistry. 2015;63(9):2525-36.
14. Picariello G, Bonomi F, Iametti S, Rasmussen P, Pepe C, Lilla S, et al. Proteomic and peptidomic characterisation of beer: Immunological and technological implications. Food Chemistry. 2011;124(4):1718-26.
15. Iimure T, Nankaku N, Hirota N, Tiansu Z, Hoki T, Kihara M, et al. Construction of a novel beer proteome map and its use in beer quality control. Food Chemistry. 2010;118(3):566-74.
16. Delvaux F, Delvaux F, Delcour J. Characterisation of the colloidal haze in commercial and pilot scale Belgian white beers. Journal of the Institute of Brewing. 2000;106(4):221-8.

Author Manuscript

This article is protected by copyright. All rights reserved.

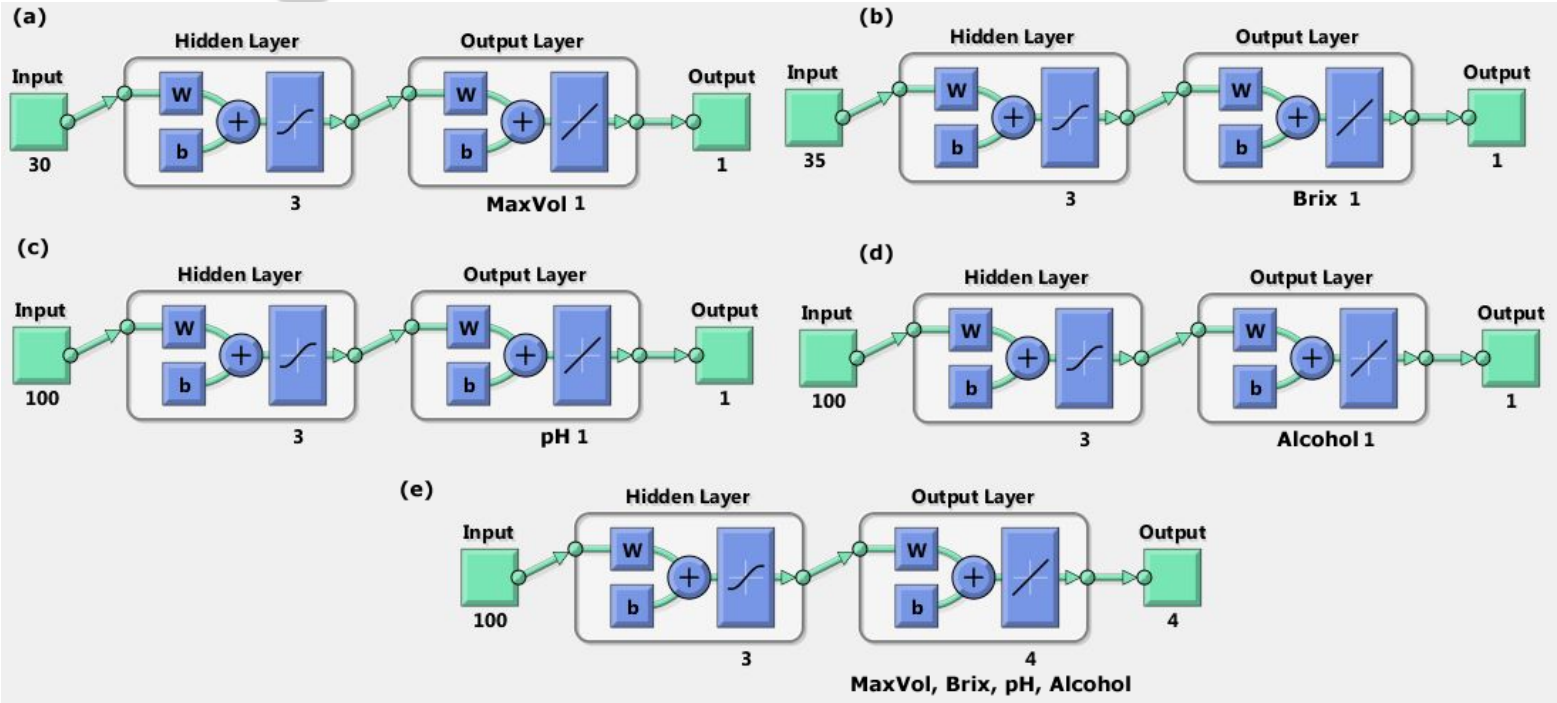
17. Cajka T, Riddellova K, Tomaniova M, Hajslova J. Recognition of beer brand based on multivariate analysis of volatile fingerprint. Journal of Chromatography A. 2010;1217(25):4195-203.
18. Iñón FA, Garrigues S, de la Guardia M. Combination of mid-and near-infrared spectroscopy for the determination of the quality properties of beers. Analytica chimica acta. 2006;571(2):167-74.
19. Zhang Y, Jia S, Zhang W. Predicting acetic acid content in the final beer using neural networks and support vector machine. Journal of the Institute of Brewing. 2012;118(4):361-7.
20. Grassi S, Amigo JM, Lyndgaard CB, Foschino R, Casiraghi E. Beer fermentation: monitoring of process parameters by FT-NIR and multivariate data analysis. Food chemistry. 2014;155:279-86.
21. Burns DA, Ciurczak EW. Handbook of near-infrared analysis: CRC press; 2007.
22. Rantanen J, Räsänen E, Antikainen O, Mannermaa J-P, Yliruusi J. In-line moisture measurement during granulation with a four-wavelength near-infrared sensor: an evaluation of process-related variables and a development of non-linear calibration model. Chemometrics and Intelligent Laboratory Systems. 2001;56(1):51-8.
23. McClure WF, Stanfield DL. Near-Infrared Spectroscopy of Biomaterials. Handbook of vibrational spectroscopy. 2002.
24. Niemet MR, Selker JS. A new method for quantification of liquid saturation in 2D translucent porous media systems using light transmission. Advances in Water Resources. 2001;24(6):651-66.
25. Ciullo PA. Industrial Minerals and Their Uses: A Handbook and Formulary: Elsevier Science; 1996.
26. Urbano-Cuadrado M, de Castro ML, Pérez-Juan P, García-Olmo J, Gómez-Nieto M. Near infrared reflectance spectroscopy and multivariate analysis in enology: Determination or screening of fifteen parameters in different types of wines. Analytica Chimica Acta. 2004;527(1):81-8.
27. Manley M, Van Zyl A, Wolf E. The evaluation of the applicability of Fourier transform near-infrared (FT-NIR) spectroscopy in the measurement of analytical parameters in must and wine. South African Journal for Enology and Viticulture. 2001;22(2):93-100.
28. Lin M-IB, Groves WA, Freivalds A, Lee EG, Harper M. Comparison of artificial neural network (ANN) and partial least squares (PLS) regression models for

This article is protected by copyright. All rights reserved.

predicting respiratory ventilation: an exploratory study. European journal of applied physiology. 2012;112(5):1603-11.
29. Bamforth CW. 125th Anniversary Review: The Non-Biological Instability of Beer. Journal of the Institute of Brewing. 2011;117(4):488-97.
30. Parpinello GP, Nunziatini G, Rombolà AD, Gottardi F, Versari A. Relationship between sensory and NIR spectroscopy in consumer preference of table grape (cv Italia). Postharvest Biology and Technology. 2013;83:47-53.
31. Abeytilakarathna P, Fonseka R, Eswara J, Wijethunga K. Relationship between total solid content and red, green and blue colour intensity of strawberry (Fragaria x ananassa Duch.) fruits. Journal of Agricultural Sciences. 2013;8(2).

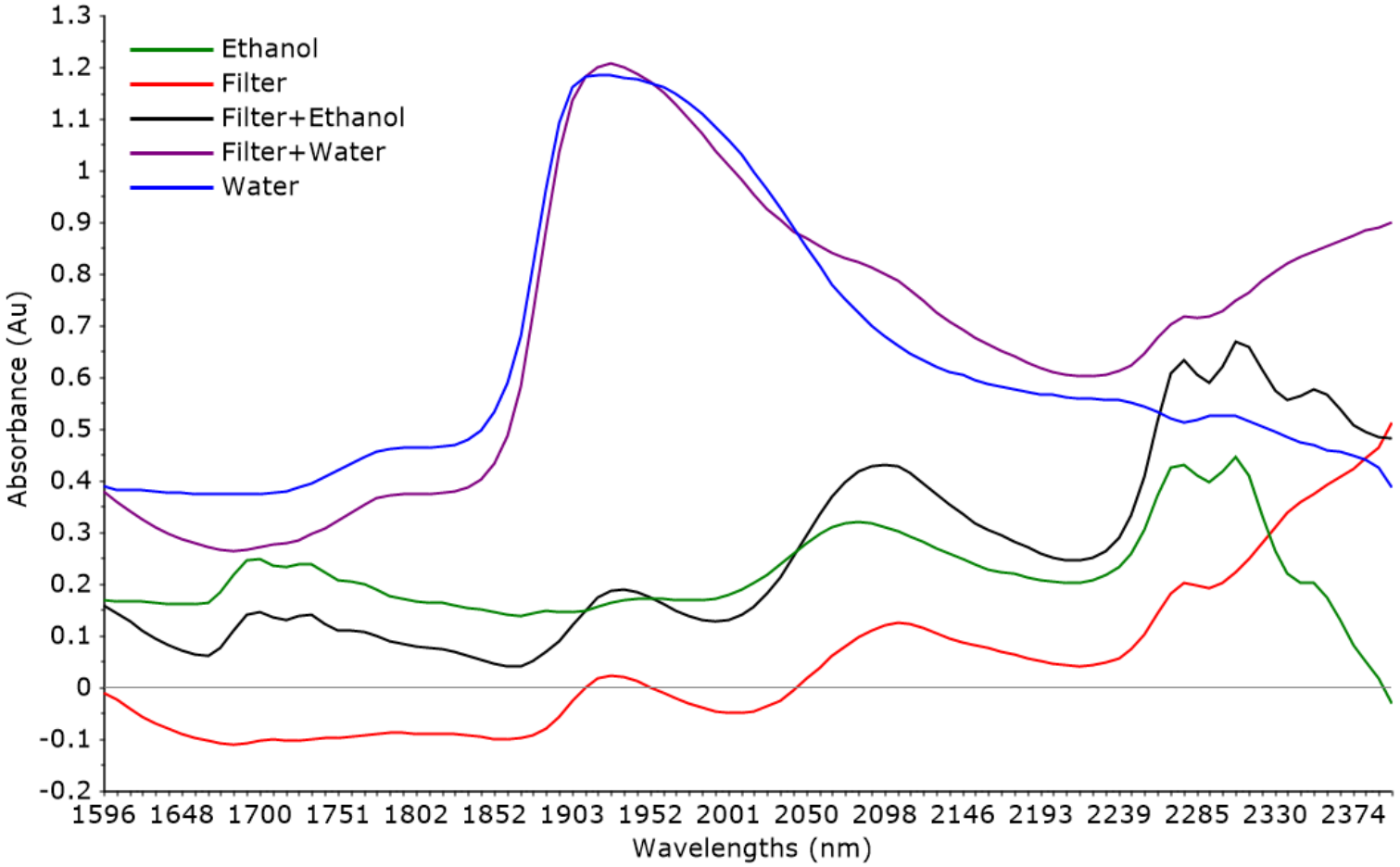
Author Manuscript

This article is protected by copyright. All rights reserved.



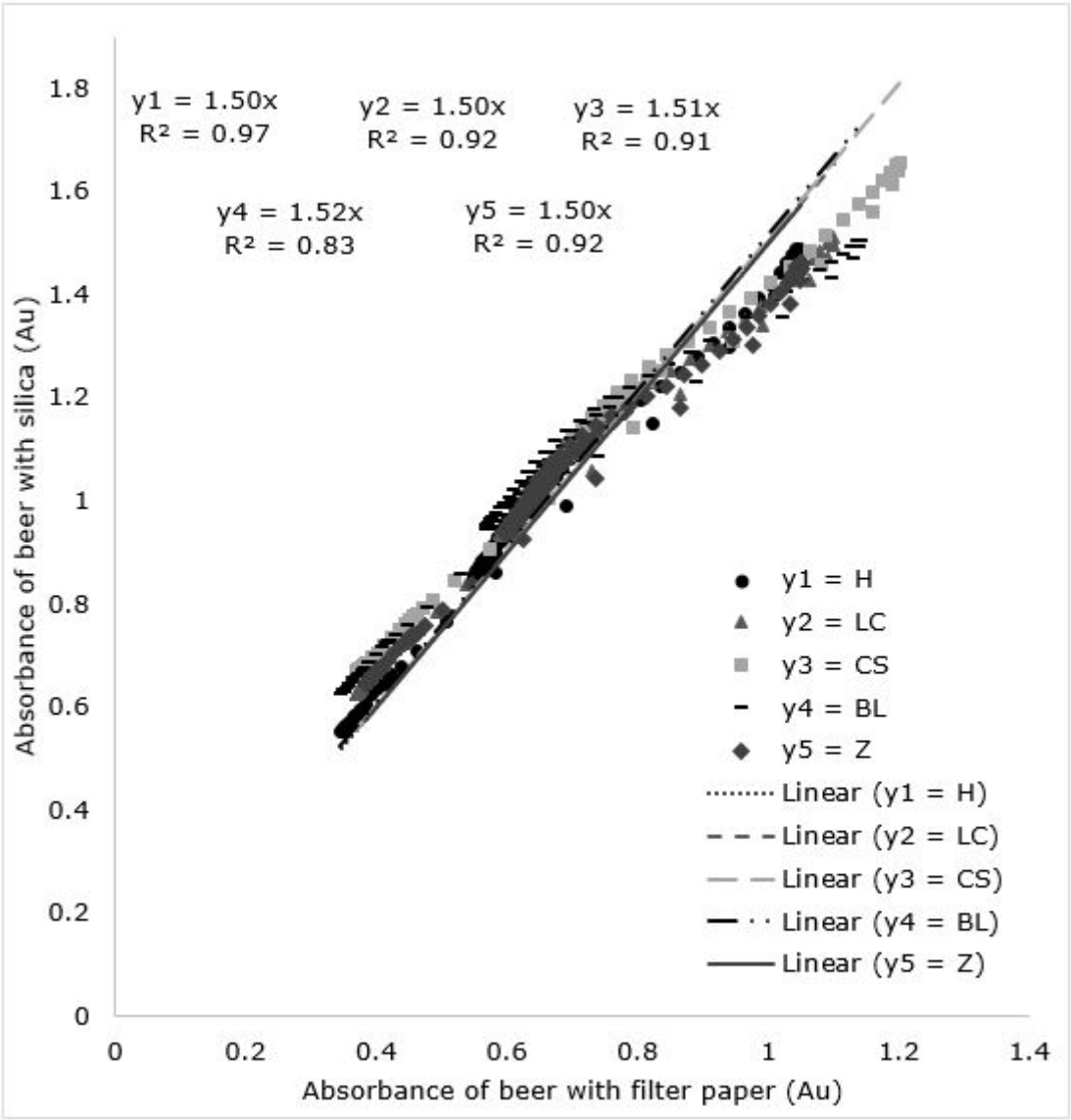
JSFA_8506_F1.tif

This article is protected by copyright. All rights reserved.



JSFA_8506_F2.tif

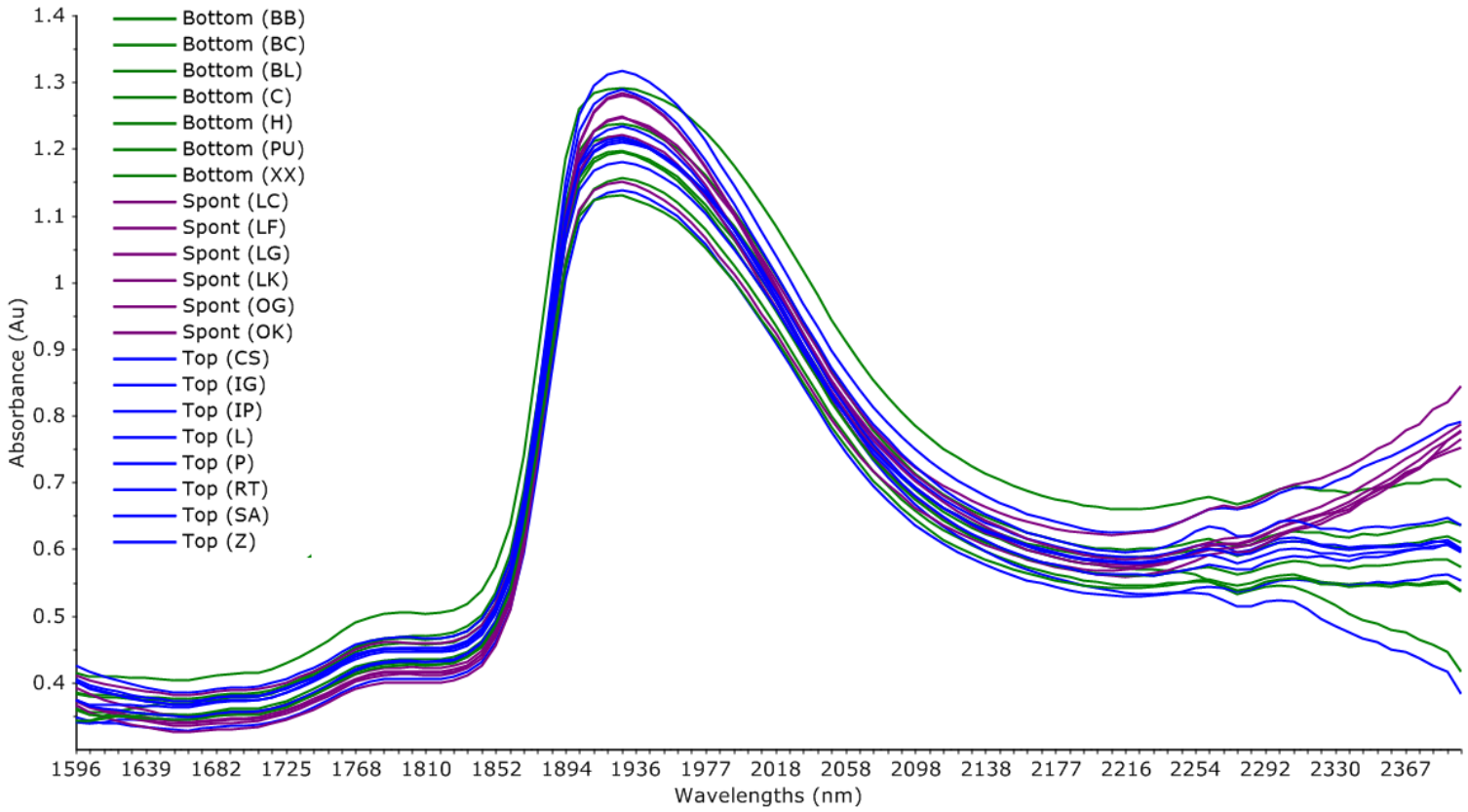
This article is protected by copyright. All rights reserved.



JSFA_8506_F3.tif

This article is protected by copyright. All rights reserved.

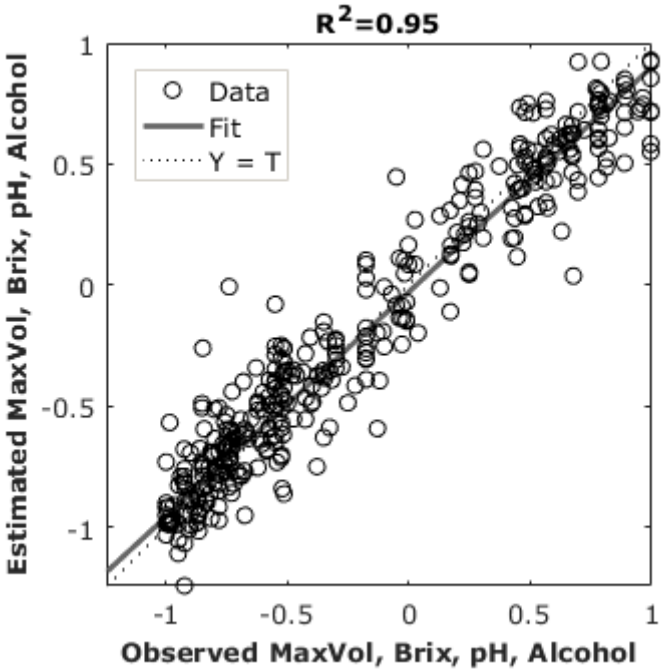
Aut ript



JSFA_8506_F4.tif

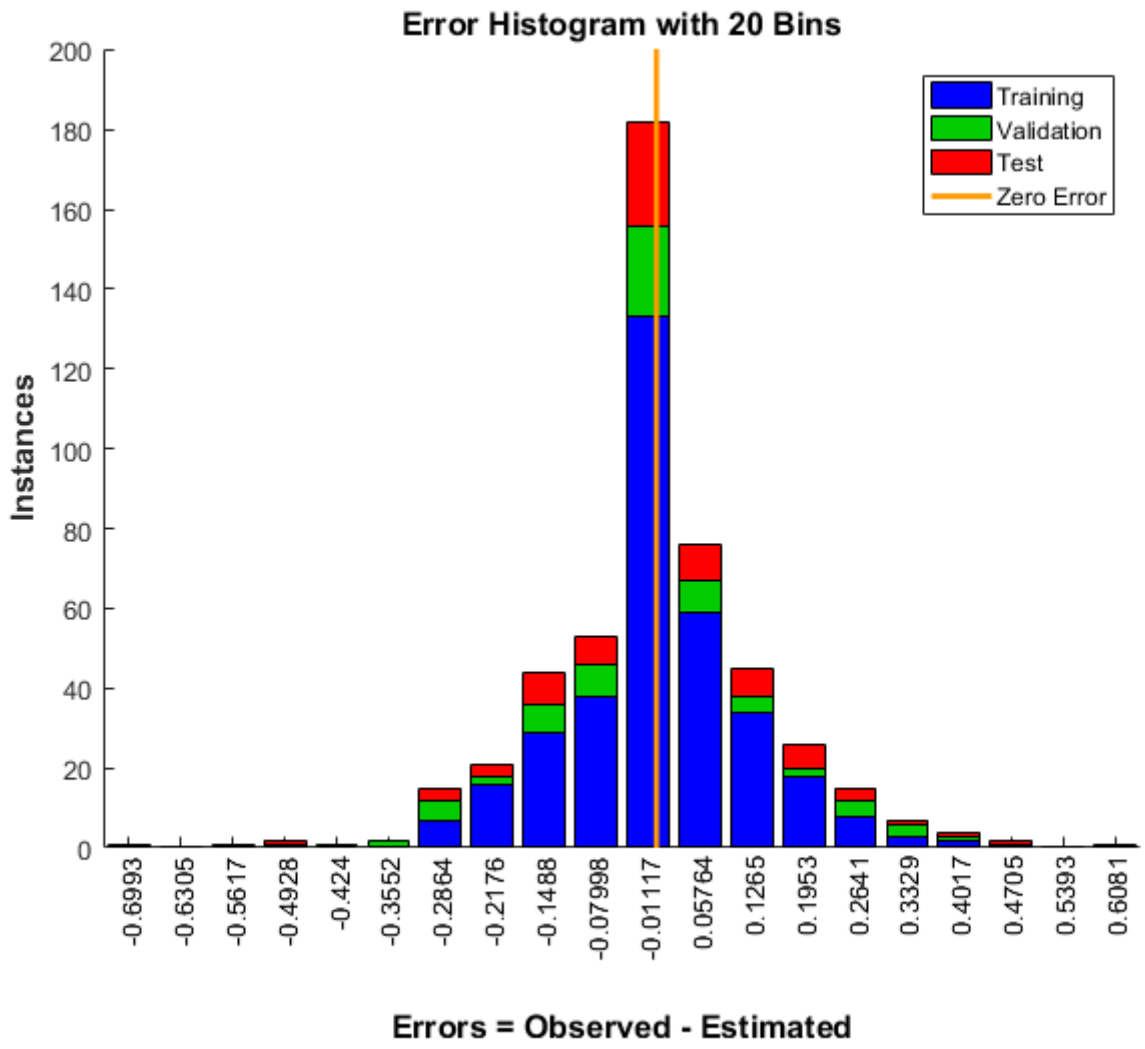
This article is protected by copyright. All rights reserved.

Author Manuscript



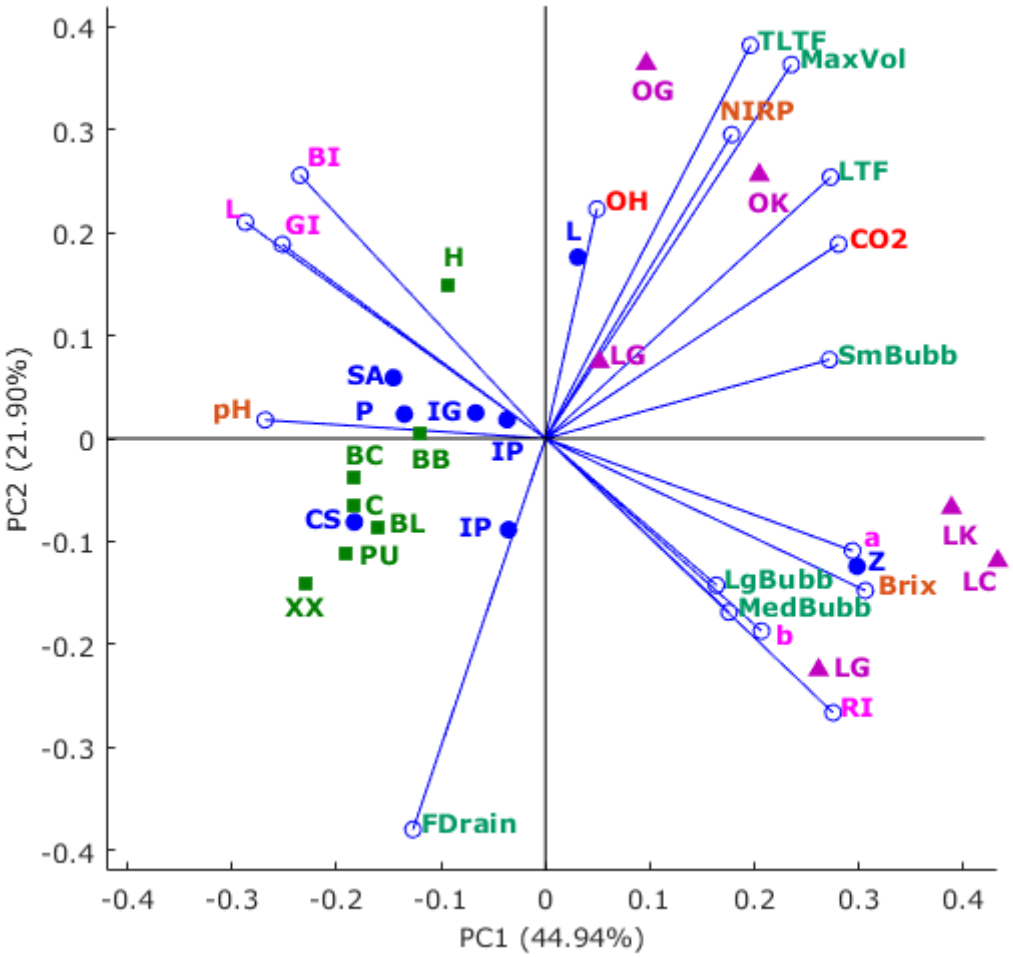
JSFA_8506_F5a.tif

This article is protected by copyright. All rights reserved.



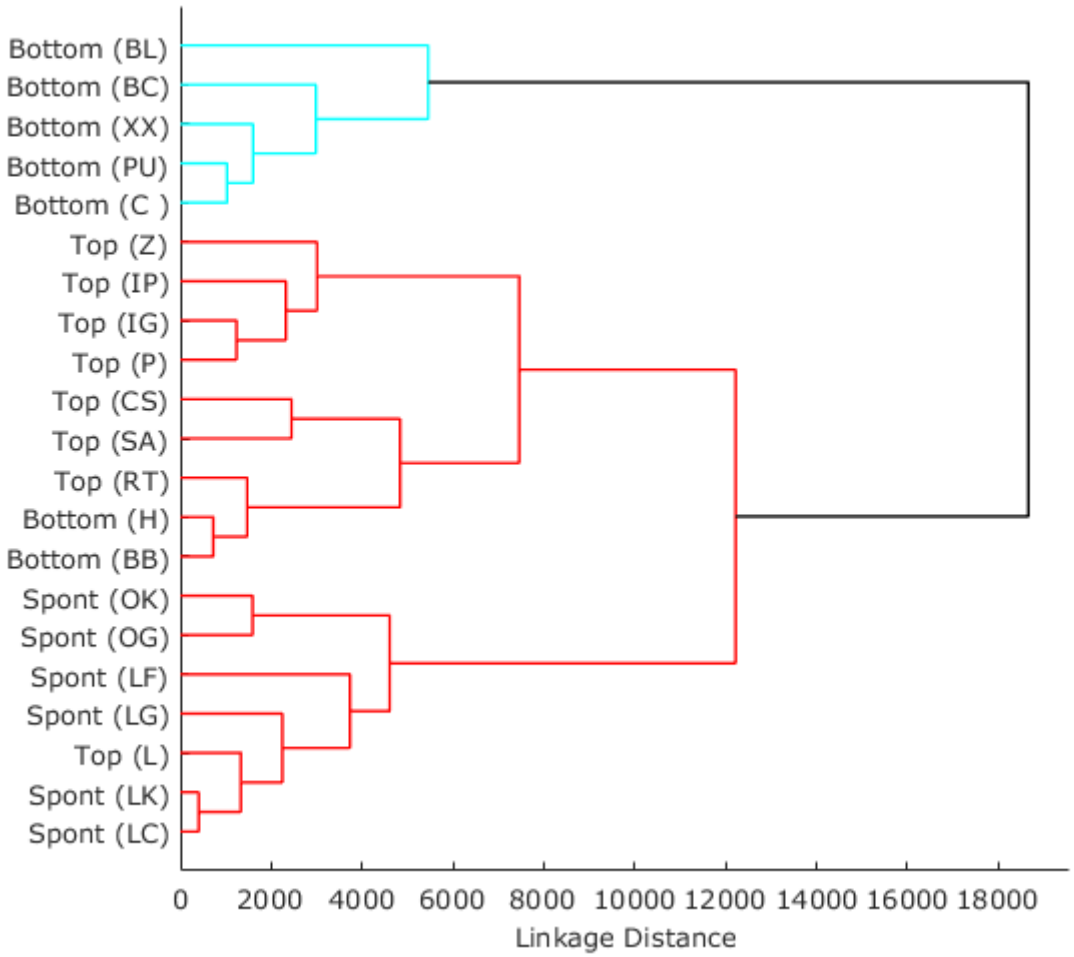
JSFA_8506_F5b.tif

This article is protected by copyright. All rights reserved.



JSFA_8506_F6a.tif

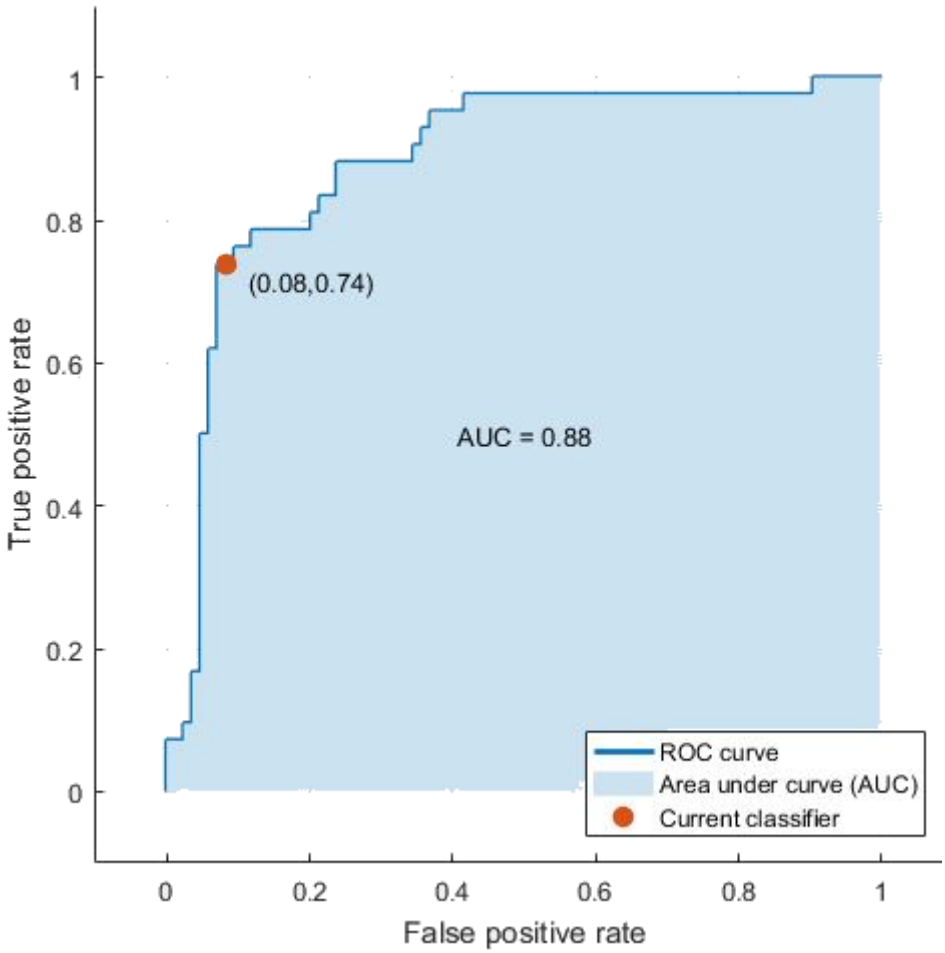
This article is protected by copyright. All rights reserved.



JSFA_8506_F6b.tif

This article is protected by copyright. All rights reserved.

Author Manuscript



JSFA_8506_F7.tif

This article is protected by copyright. All rights reserved.